

Western Kentucky University

TopSCHOLAR®

---

Mahurin Honors College Capstone Experience/  
Thesis Projects

Mahurin Honors College

---

2021

## Synthesis and Catalytic Properties of Metal-Organic Frameworks Mimicking Carbonic Anhydrase

Longji Li

Western Kentucky University, longji.li962@topper.wku.edu

Follow this and additional works at: [https://digitalcommons.wku.edu/stu\\_hon\\_theses](https://digitalcommons.wku.edu/stu_hon_theses)



Part of the [Chemistry Commons](#), and the [Materials Science and Engineering Commons](#)

---

### Recommended Citation

Li, Longji, "Synthesis and Catalytic Properties of Metal-Organic Frameworks Mimicking Carbonic Anhydrase" (2021). *Mahurin Honors College Capstone Experience/Thesis Projects*. Paper 924.  
[https://digitalcommons.wku.edu/stu\\_hon\\_theses/924](https://digitalcommons.wku.edu/stu_hon_theses/924)

This Thesis is brought to you for free and open access by TopSCHOLAR®. It has been accepted for inclusion in Mahurin Honors College Capstone Experience/Thesis Projects by an authorized administrator of TopSCHOLAR®. For more information, please contact [topscholar@wku.edu](mailto:topscholar@wku.edu).

SYNTHESIS AND CATALYTIC PROPERTIES OF METAL-ORGANIC  
FRAMEWORKS MIMICKING CARBONIC ANHYDRASE

A Capstone Experience/Thesis Project Presented in Partial Fulfillment  
of the Requirements for the Degree Bachelor of Science  
with Mahurin Honors College Graduate Distinction  
at Western Kentucky University

By:

Longji Li

May 2021

\*\*\*\*\*

CE/T Committee

Dr. Bangbo Yan

Dr. Cathleen Webb

Dr. Matthew Nee

Copyright by

Longji Li

2021

## ABSTRACT

The natural enzyme carbonic anhydrase has gained attention in recent years for its ability to catalyze the interconversion of aqueous carbon dioxide (CO<sub>2</sub>) and bicarbonate. However, it lacks the efficiency to qualify practical usage on a large scale due to its inherent deficiency and fragile nature. On the other hand, its active center can be used as an ideal model for the design of novel catalytic materials targeting carbon dioxide capture and sequestration. This study focused on the synthesis of a zinc-based metal-organic framework (Zn-MOF-1) mimicking the carbonic anhydrase using the solvothermal method. Important properties such as catalytic ability, thermal stability, and reusability were investigated as well. Zn-MOF-1 demonstrated the ability to catalyze the *para*-nitrophenyl acetate hydrolysis, the thermal stability up to 400 °C, and the high reusability in basic solutions. These results suggested that the Zn-MOF-1 can be potentially applied to CO<sub>2</sub> conversion.

## ACKNOWLEDGEMENTS

I would first like to thank my research advisor Professor Bangbo Yan for his continuous guidance and great support. I would like to thank Professor Cathleen Webb and Professor Matthew Nee for serving on my thesis committee and as my thesis readers, and for their valuable suggestions. I would like to acknowledge my colleagues Mrs. Simrat Kaur and Mrs. Mary Begley for their help on the synthetic methods and infrared spectroscopy. I would also like to thank Ms. Pauline Norris, who is the manager of Advanced Materials Institute, for her assistance with thermogravimetric analysis and elemental analysis. Finally, I would like to thank my parents for guiding me in the right direction and being there for me without a doubt.

## VITA

### *EDUCATION*

Western Kentucky University, Bowling Green, KY May 2021

B.S. in Chemistry – Mahurin Honors College Student

Honors CE/T: *Synthesis and catalytic properties of metal-organic frameworks  
mimicking carbonic anhydrase*

The Gatton Academy of Mathematics and Science, Bowling Green, KY May 2017

South Warren High School, Bowling Green, KY May 2017

### *AWARDS & HONORS*

Cum Laude, WKU, May 2021

Undergraduate Award in Inorganic Chemistry, WKU, May 2020

Gower Endowed Scholarship Fund, WKU, 2018-2019.

Named to the Dean's List, WKU, 2017-2021.

Cornelius A Martin Scholarship, WKU, 2017-2021.

## CONTENTS

|                              |     |
|------------------------------|-----|
| Abstract.....                | ii  |
| Acknowledgments.....         | iii |
| Vita.....                    | iv  |
| List of Figures.....         | vi  |
| Introduction.....            | 1   |
| Experimental Procedures..... | 7   |
| Results.....                 | 10  |
| Discussion.....              | 17  |
| Conclusion.....              | 21  |
| References.....              | 22  |

## LIST OF FIGURES

|                                                                                              |    |
|----------------------------------------------------------------------------------------------|----|
| Figure 1. The tetrahedral Zn <sup>2+</sup> center in carbonic anhydrase and imidazole.....   | 2  |
| Figure 2. Lipscomb and Lindskog mechanisms for the rearrangement of<br>the intermediate..... | 3  |
| Figure 3. Structure of L-histidine.....                                                      | 5  |
| Figure 4. The decomposition of <i>p</i> -NPA.....                                            | 6  |
| Figure 5. FTIR spectrum of ZnMOF-1.....                                                      | 11 |
| Figure 6. Calibration curve of <i>p</i> -NP.....                                             | 12 |
| Figure 7. Catalytic analysis of ZnMOF-1.....                                                 | 12 |
| Figure 8. TGA curve of ZnMOF-1.....                                                          | 14 |
| Figure 9. XRD patterns of ZnMOF-1 before and after catalysis.....                            | 16 |



## INTRODUCTION

Over the last few decades, human emissions of greenhouse gases such as carbon dioxide (CO<sub>2</sub>) have increased significantly and are a primary driver of climate change, which presents one of the world's most pressing challenges.<sup>1</sup> Therefore, it is urgent to develop effective methods to capture CO<sub>2</sub> and mitigate CO<sub>2</sub> emissions. Biological CO<sub>2</sub> sequestration based on enzymes has demonstrated great potential because of its environmentally friendly nature. This method has great sustainability in terms of regulating the atmospheric carbon dioxide level and helping to reduce the greenhouse effect. However, the application of natural enzymes has often been limited due to its inherent deficiency caused by its high sensitivity to pH, slow carbonation rate, low thermal stability, and high cost.<sup>2</sup> Hence, biological sequestration will not be practical for the economic industrial process unless these critical problems are solved. Our approach is to develop new materials to simulate the properties of carbonic anhydrase (CA).

CA plays an important role in the mammalian tissues, plants, algae, and bacteria. It is a family of enzymes that catalyze the interconversion from CO<sub>2</sub> and water to the dissociated ions of carbonic acid. The equilibrium position of this reaction is pH-dependent. Hydration of CO<sub>2</sub> takes place when pH<7, and the dehydration of bicarbonate predominates when pH>7.<sup>3</sup> Thus, the ideal environment of the catalysis should be consistent in pH. The CA's family consists of three distinct classes (alpha, beta, and gamma). CA from mammals belongs to the alpha class, the plant enzymes belong to the beta class, and the enzymes from methane-producing bacteria belong to the gamma class.

Members of these different classes share very little sequence or structural similarity, yet they all perform the same function and rely on a zinc ion at the active site.<sup>4</sup>

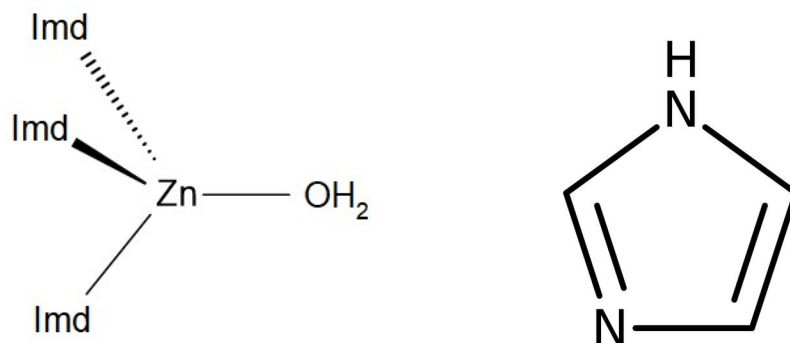


**Figure 1.** The tetrahedral  $Zn^{2+}$  center in carbonic anhydrase (left) and imidazole (right)

As Figure 1 indicates, the active site contains a tetrahedral  $Zn^{2+}$  center, which coordinates three nitrogen atoms from the imidazole group and an aqua ligand on the fourth coordination site. Histidine residues on the active site increase the Lewis acidic character of the central  $Zn^{2+}$  metal ion by withdrawing electron clouds towards themselves.<sup>4</sup> The structure of the active center allows CA to perform a nucleophilic attack from a zinc-hydroxyl group toward  $CO_2$ , forming bicarbonate anions (Figure 2). Brauer<sup>5</sup> et al. studied the mechanism of intramolecular proton shifts in individual steps of the catalytic reactions. Specifically, the zinc-bonded oxygen attacked carbon dioxide, and the formation of bicarbonate is followed by either an intramolecular proton transfer (Lipscomb mechanism) or an internal rotation of the bicarbonate (Lindskog mechanism).

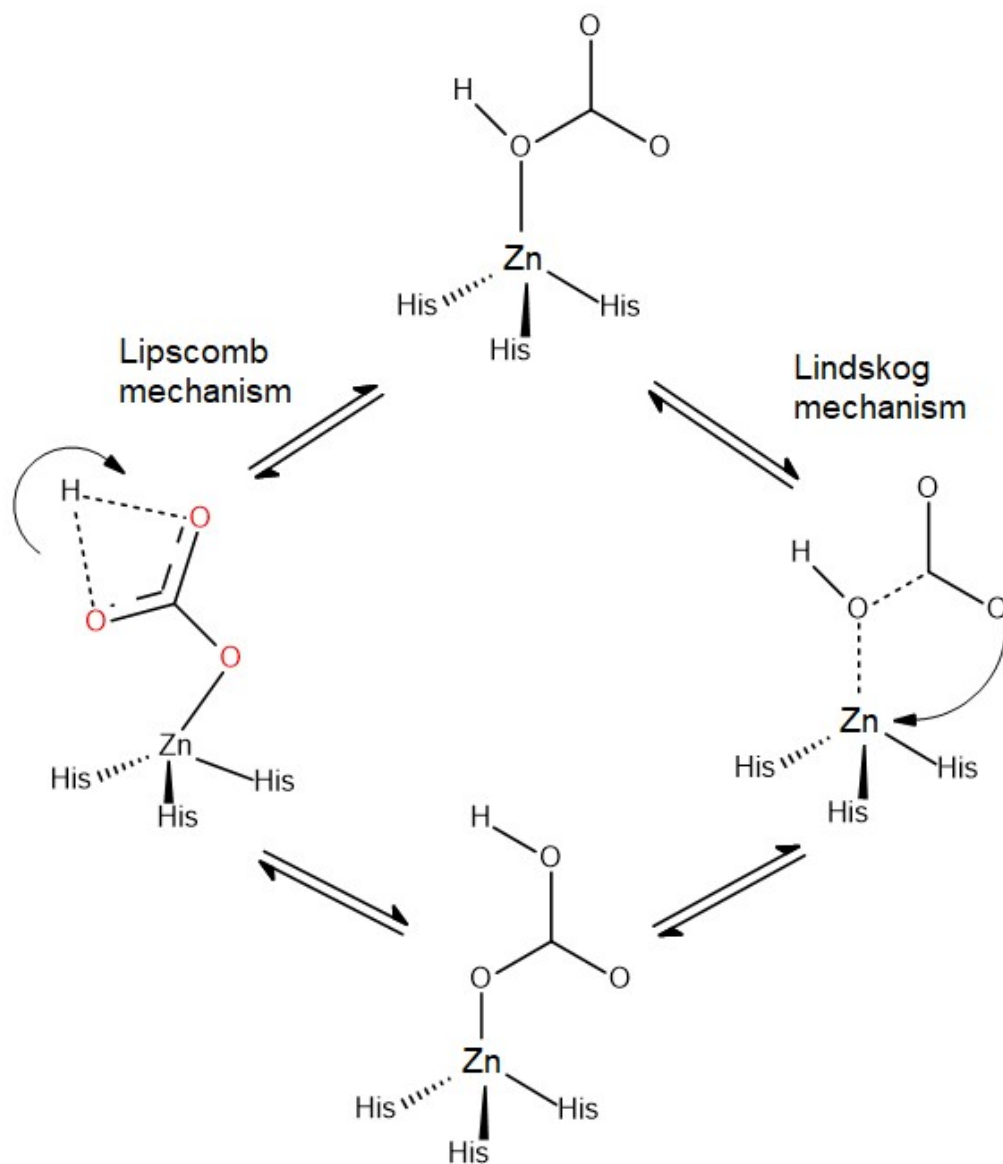


**Figure 2.** Lipscomb and Lindskog mechanisms for the rearrangement of the intermediate<sup>5</sup>

Density functional theory calculations and computer simulations indicated that the intermediate tends to form the Lindskog product first. However, due to its kinetic instability, a rotation about the CO<sub>2</sub> bond axis to yield the Lipscomb product takes place instead. This

process is comparably faster than the hydration of aqueous CO<sub>2</sub>. Thus, the formation of the intermediate is generally considered as the rate-limiting step for CO<sub>2</sub> uptake.<sup>6,7</sup>

Inspired by the structural and catalytic properties of CA, our focus for this project is to design and synthesize a metal-organic framework (MOF) containing a metal center that mimics the active centers of CA. Metal-organic frameworks (MOFs) are a class of compounds consisting of metal ions or clusters coordinated to organic ligands to form porous structures. Because MOFs are hybrids of organic and inorganic structures, they are an excellent platform for mimicking CA's active center while having a robust open framework.<sup>2</sup> Additionally, MOFs are featured with versatile structures, high surface area, and tunable porosity. These properties grant MOFs great potential to be customized and designed for certain coordination. Combining the features of MOFs and CA, we expect to simulate the structures of natural CA using specially designed MOFs that can perform the same catalytic ability but with better efficiency.

In fact, some researchers have studied the catalytic properties of Zn-based MOFs on CO<sub>2</sub> conversion. For instance, Jin<sup>8</sup> et al. synthesized CFA-1 and ZIF-100 to mimic CA to convert CO<sub>2</sub> gas into carbonate. These compounds exhibited excellent reusability, solvent, and thermal stability. Huang<sup>9</sup> et al. developed a nonanuclear zinc coordination complex that possesses an even better performance than CFA-1. Pan<sup>10</sup> et al. developed a rapid synthesis of ZIF-8 using Zn(NO<sub>3</sub>)<sub>2</sub> and 2-methylimidazole. However, there are no reports on using histidine as a ligand in the synthesis of MOFs to mimic the properties of CA.

In addition to synthesizing Zn-based MOFs, incorporating CA within MOFs via co-precipitation has been investigated. For instance, Ren<sup>11</sup> et al. assembled CA@ZIF-8

nanocomposites to a membrane that captures CO<sub>2</sub> sequestration. Moreover, small molecules containing Zn mimicking CA have also been studied. For example, Floyd<sup>12</sup> et al. reported the catalytic activity of a zinc cyclen molecule under rigorous conditions resembling an industrial process. Naturally, enzymes work best at room temperature and atmospheric pressure, and especially strict with ambient pH values. Zinc cyclen, however, showcased unusual durability against these conditions. It was also found that the catalytic activity of zinc cyclen increased with increasing temperature (100-130 °C) and pH (>12). However, its activity is diminished at pH<9.

In this study, we chose Zn(NO<sub>3</sub>)<sub>2</sub> as the source of active centers, not only because the vast majority of CA are zinc-based, but also due to the ideal nature of zinc in coordination chemistry. Comparing to cadmium, a less common active center for CA, zinc is more prone to have a coordination number of 4, especially with ionized ligands. L-histidine was used as the source of imidazole nitrogen. Figure 3 shows that L-histidine consists of an imidazole side chain, a primary amine, and a carboxylic acid group. The structure of L-histidine has the potential to repeat coordination entities in two or three dimensions.

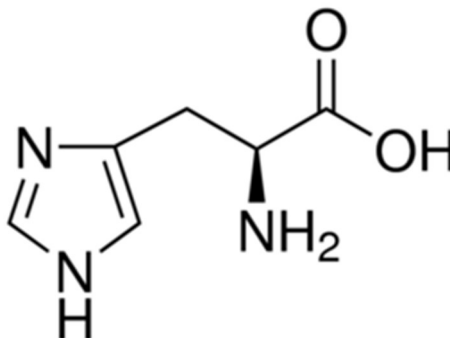


**Figure 3.** Structure of L-histidine

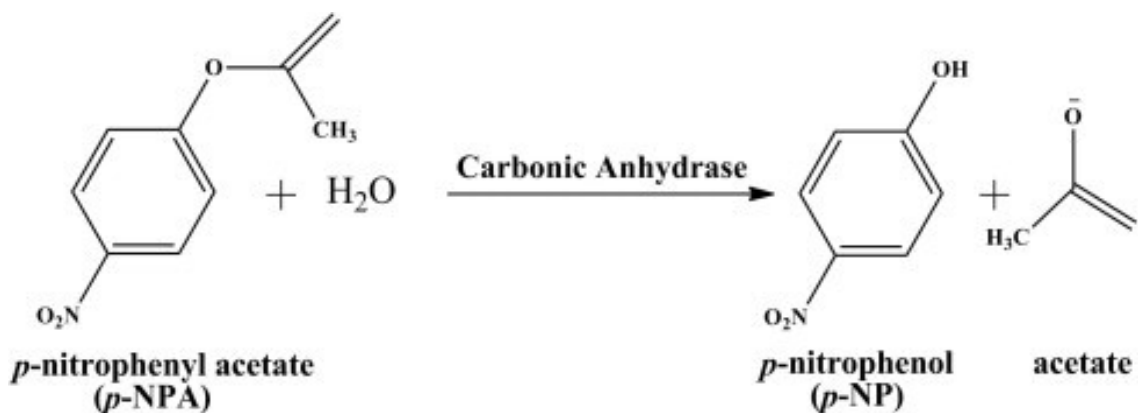


**Figure 4.** The decomposition of *p*-NPA

The catalytic activity of the new material was studied using the self-decomposition reaction of *para*-nitrophenyl acetate (*p*-NPA). As Figure 4 demonstrates, under room temperature and atmospheric pressure, *p*-NPA can gradually turn into its hydrolyzed product *para*-nitrophenol (*p*-NP). Because this reaction can also be catalyzed by CA, utilizing a UV/vis spectrometer to monitor the concentration changes of *p*-NP over time with the addition of synthesized product becomes a viable method to determine whether the material has the catalytic activity.<sup>9</sup>

## EXPERIMENTAL PROCEDURES

### Materials

L-histidine monohydrochloride monohydrate ( $C_6H_9N_3O_2 \cdot HCl \cdot H_2O$ ,  $M_w$ : 209.63), potassium hydroxide, and zinc nitrate hexahydrate, 99% ( $Zn(NO_3)_2 \cdot 6H_2O$ ,  $M_w$ : 297.47) were purchased from Alfa Aesar. Deionized (DI) water was used in all experiments. All the reagents were analytical grade and were used without further purification.

### Synthesis of ZnMOF-1

In a PTFE cup,  $Zn(NO_3)_2 \cdot 6H_2O$  (594 mg, 2.00 mmol) and L-histidine (253 mg, 1.21 mmol) were dissolved with DI water (10 mL). To the resulting solution, 8 mL of 0.5 M KOH solution was added. The solution became cloudy immediately. After a thorough stirring, the reaction mixture was then sealed in a steel autoclave and heated at 130 °C for 48 hours in an oven. The white solids were filtered and washed with DI water three times. After dried in the air, 47.4 mg (yield 10.9% based on L-histidine) of products were obtained.

### Powder X-ray diffraction

The X-ray diffraction pattern of the synthesized material was obtained from a Bruker AXS D2 Phaser diffractometer. Approximately 20 mg of the sample was used. Scattering angle  $2\theta$  ranged from 10° to 50° with an increment of 0.01°. The initial PSD was set to 4.5°.

## **Infrared spectroscopy**

The infrared spectra of ZnMOF-1 were recorded on a Fourier-transformed infrared spectrometer (Perkin Elmer Spectrum 100) in the 4000-400  $\text{cm}^{-1}$ .

## **Thermogravimetric analysis**

The thermal stability of ZnMOF-1 was run on an STA 449 F1 Jupiter thermal analyzer with samples held in platinum pans in a continuous flow nitrogen atmosphere at the rate of 20 mL/min. Samples were heated at a constant rate of 10°C/min from room temperature to 800°C.

## **Elemental analysis**

The C, H, and N elemental analyses of ZnMOF-1 were carried out on the Flash 2000 Elemental Analyzer.

## **Biomimetic catalysis study**

The catalytic activity of ZnMOF-1 was examined by coupling with the hydrolysis reaction of *p*-NPA.

### 1. Preparation of HEPES buffer (50 mM, pH 8.0)

HEPES (4-(2-hydroxyethyl)-1-piperazineethanesulfonic acid) buffer was prepared by dissolving 5.96 g of HEPES in 400 mL of DI water. The pH of the solution was measured with a pH meter. KOH pellets were added to the solution until its pH reached 8. Then, the solution was transferred into a 500 mL of volumetric flask. DI water was added up to the mark of 500 mL.



## 2. The *p*-NP calibration curve

The calibration curve for *p*-NP concentrations was plotted by UV-vis absorptions at 402 nm for various known concentrations (5, 10, 25, 50, 100  $\mu$ M) of *p*-NP. The *p*-NP solutions were prepared using HEPES buffer (50 mM, pH 8.0).

## 3. Assay of activities of the ZnMOF-1

In a 100 mL beaker, 4.9 mg of *p*-NPA was dissolved in 2.5 mL of acetonitrile. Then, 47.5 mL of HEPES buffer, and 10 mg of MOF were added to this solution. The absorbance at 402 nm of the mixture was measured with a UV-vis spectrometer every 5 minutes for 2 hours. The blank control was carried out under the same conditions without adding the ZnMOF-1 catalyst. This can be used to determine the reaction rate of self-decomposition of the *p*-NPA, and as a reference to the rate of the decomposition of the *p*-NPA catalyzed by ZnMOF-1.

### **Stability of zinc coordination compound in buffer solution.**

To determine if the catalyst can be recycled after the reaction, the stability of ZnMOF-1 in HEPES buffer (50 mM, pH 8.0) was evaluated. 47.4 mg of the catalyst was added to 20.0 mL of HEPES buffer (50 mM, pH 8.0). The mixture was stirred at room temperature for 2 hours. Subsequently, the solids were separated by centrifugation and dried at 120 °C for 12 hours for PXRD analysis.

## RESULTS

### **Synthesis**

Hydrothermal (using water as the solvent) reactions of  $\text{Zn}(\text{NO}_3)_2 \cdot 6\text{H}_2\text{O}$  with L-histidine have led to the formation of a white solid product (ZnMOF-1), while solvothermal reactions of anhydrous  $\text{Zn}(\text{NO}_3)_2$  with L-histidine (using methanol as the solvent) have led to an orange solid product. PXRD patterns of both products were obtained. The orange product exhibited very weak X-ray diffractions. Thus, no further studies on it were performed.

### **Infrared spectrum**

The infrared spectrum of ZnMOF-1 was shown in Figure 5. This spectrum provided us important information on functional groups. Following bands are observed: N-H stretching at  $3225\text{ cm}^{-1}$ , O-H stretching at  $3195\text{ cm}^{-1}$ , cyclic C=C stretching at  $1581\text{ cm}^{-1}$ , carboxylate bending at  $1451\text{ cm}^{-1}$ , and Zn-O stretching at  $664\text{ cm}^{-1}$ .<sup>13</sup>

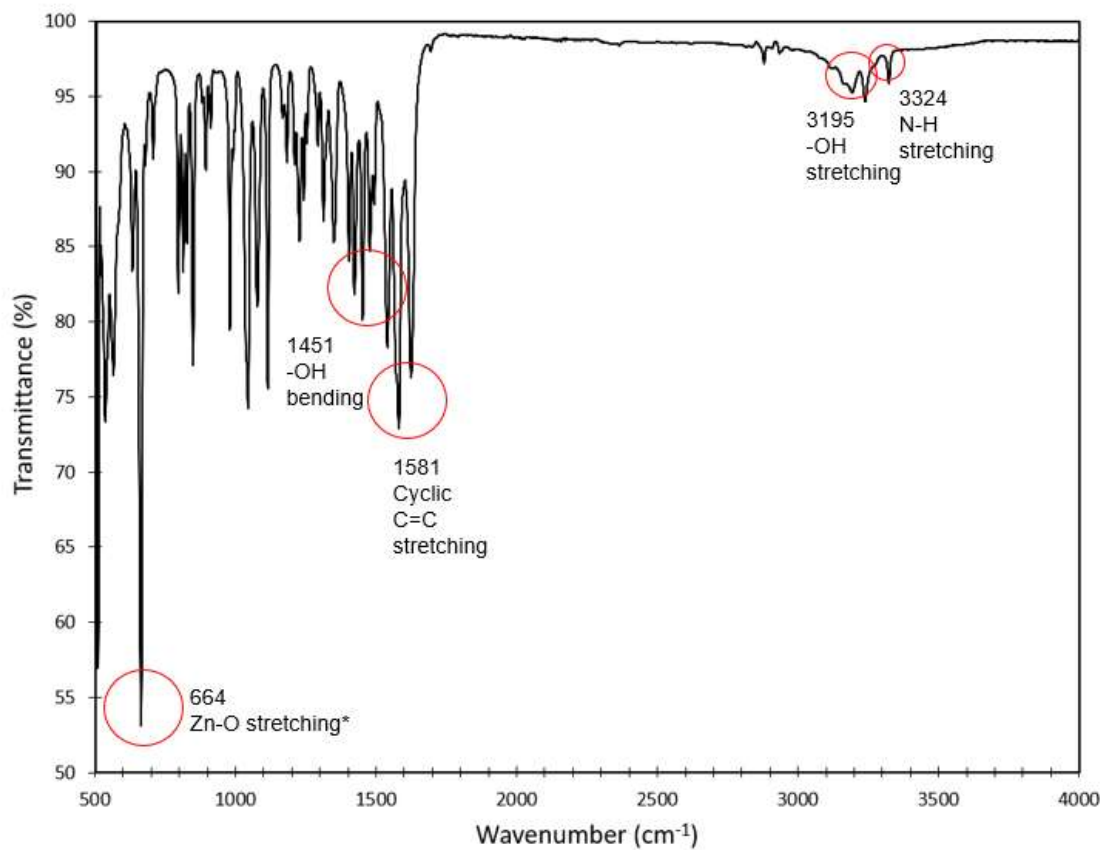


**Figure 5.** FTIR spectrum of ZnMOF-1

### Catalytic study

A calibration curve was prepared with stock *p*-NP solutions at 5, 10, 25, 50, and 100 mM (Figure 6).

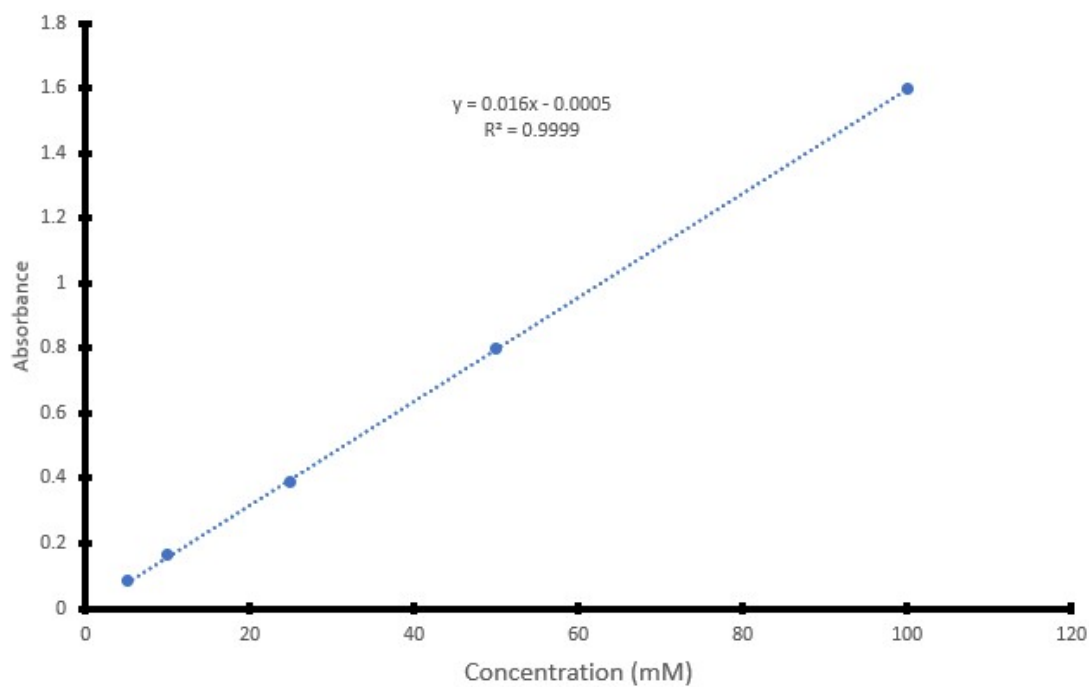


**Figure 6.** Calibration curve of *p*-NP

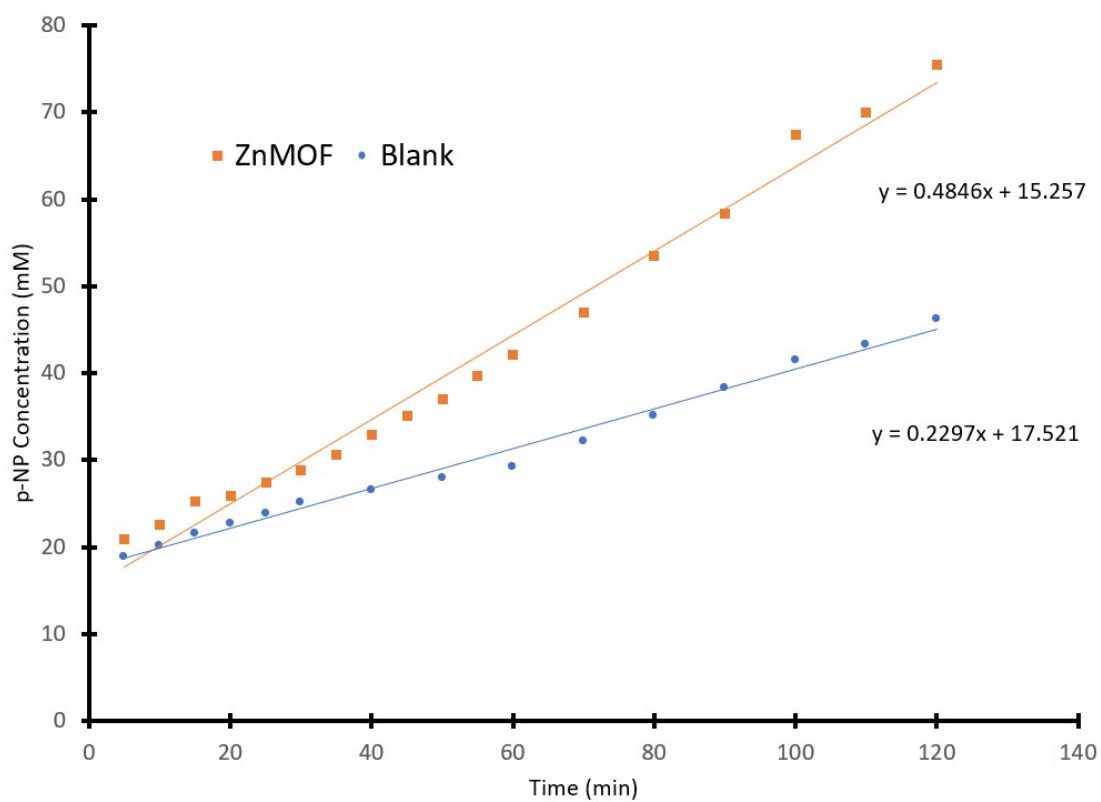


**Figure 7.** Catalytic analysis of ZnMOF-1

The results of the catalytic activities of ZnMOF-1 on *p*-NPA hydrolysis were shown in Figure 7. The blue line represented *p*-NP solution concentration changes with time under the catalysis of ZnMOF-1, and the orange line represented the *p*-NP concentration changes without adding the ZnMOF-1 catalyst. In both cases, the concentration of *p*-NP and reaction time show a linear relationship. However, the reaction catalyzed by ZnMOF-1 shows a steeper slope of the *p*-NP concentration-time plot (blue line). After 2 hours of reaction, the reaction catalyzed by ZnMOF-1 had a *p*-NP concentration 63% higher than the reaction without the catalyst. The reaction rate of catalyzed solution is 2.1 times that of the blank control. These results demonstrated that ZnMOF-1 can mimic the functions of CA and catalyzed the *p*-NPA hydrolysis reaction.

### **Thermal stability**

4.395 mg of ZnMOF-1 was analyzed with TGA to evaluate its thermal stability (Figure 8), and a 60% loss of weight was observed.

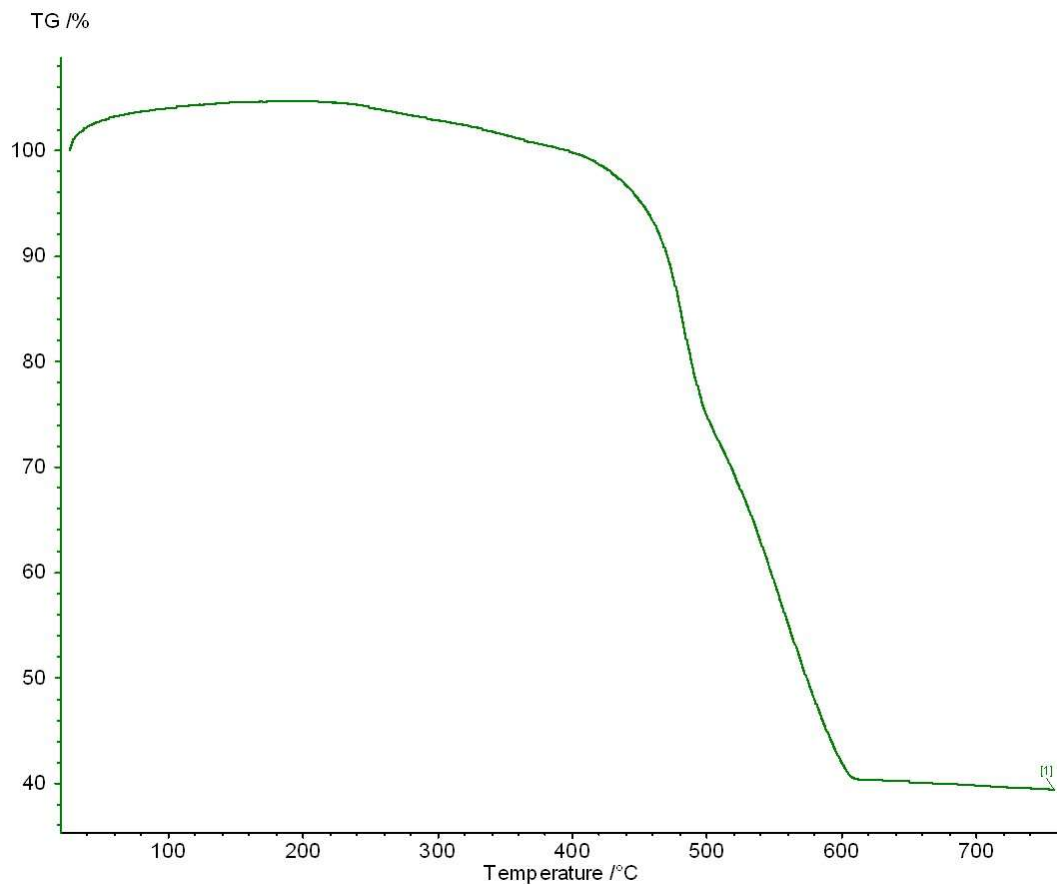


**Figure 8.** TGA curve of ZnMOF-1

As the TGA plot indicated, at 400 °C, the sample started to have a significant loss of mass. It can be attributed to the removal and the decomposition of the organic ligand in ZnMOF-1. Around 500 °C, the TGA curve suggested the decomposition of the organic ligand and the possible formation of zinc oxide. The residue of the TGA shows a white color, indicating the formation of zinc (II) oxide.

### **Elemental analysis**

The average percentages of the three samples for ZnMOF-1 were 17.9% N, 32.1% C, and 3.3% H. These values are close to the theoretical values 19.2% N, 32.9% C, and 3.23% H for ZnMOF-1 (Empirical formula:  $\text{ZnC}_6\text{H}_7\text{N}_3\text{O}_2$ ).

### **Stability of zinc coordination compound in buffer solution**

After stirred for 2 hours in HEPES buffer (pH=8) solution, ZnMOF-1 was retrieved by centrifuging the solution and drying it in an oven. 36.2 mg of ZnMOF-1 was recycled from 47.4 mg input, which leads to a 76% recycling rate. PXRD pattern was recorded for the recovered ZnMOF-1 and compared to the one before catalytic analysis. As Figure 9 shows, their patterns match very well, indicating no major change of the structure for ZnMOF-1 took place in the buffer solution.

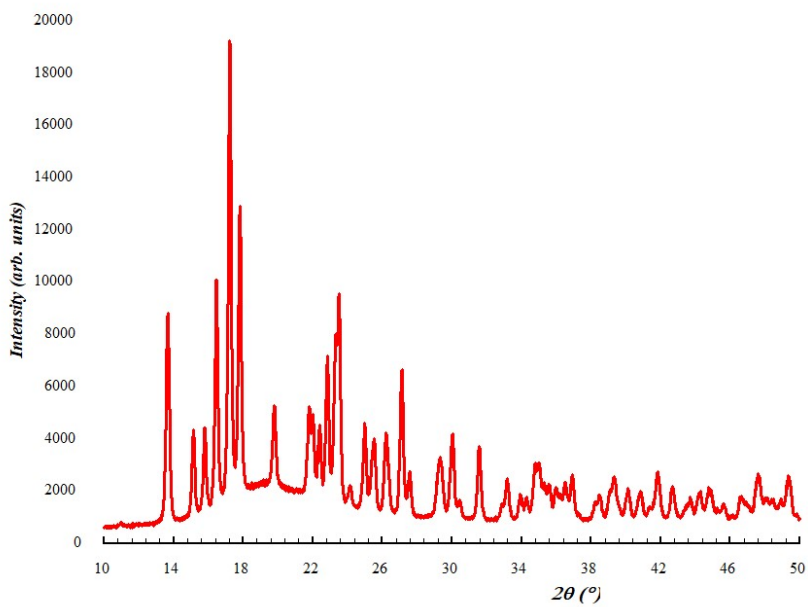
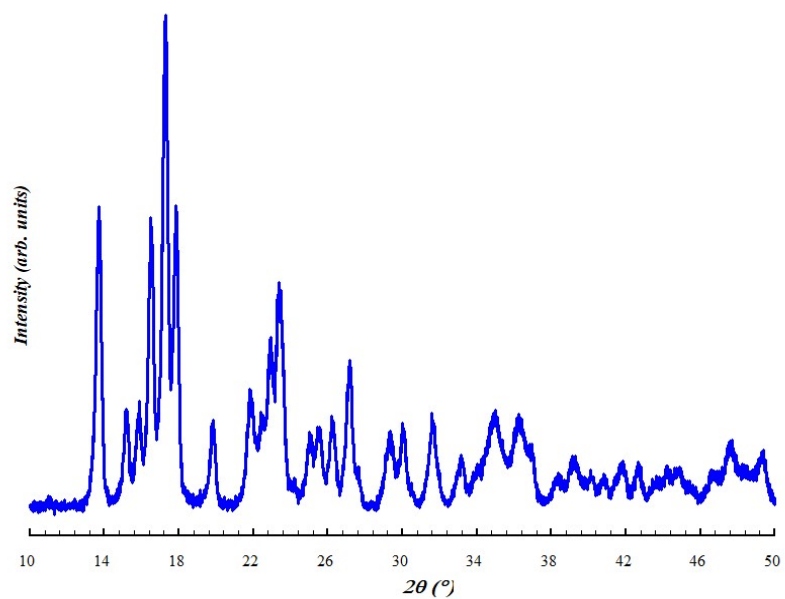


**Figure 9.** XRD patterns of ZnMOF-1 before(top) and after(bottom) catalysis



## DISCUSSION

The focus of this study is synthesizing metal-organic frameworks that can mimic the catalytic properties of CA. The features of MOFs can make up for the disadvantages of CA so that the biomimetic MOFs can be broadly used under more practical conditions. Herein, we have successfully made a zinc-based MOF (ZnMOF-1) using  $\text{Zn}(\text{NO}_3)_2 \cdot 6\text{H}_2\text{O}$  and L-histidine as starting materials. KOH solution was used to adjust the pH of the reaction mixture and to neutralize the hydrogen ions formed in the synthesis.

Successful synthesis of ZnMOF-1 involves several factors such as reactant concentrations, molar ratios, reaction temperature, pH, and reaction time. Sometimes, even the order of adding reactants to the reaction vessels can significantly affect the results. Thus, several changes in reaction conditions were carried out throughout this study to grow big crystals and to increase the yield of the product. For example, the pH of the reaction mixture was adjusted with KOH. Because L-histidine is a weak acid, the formation of the MOF from L-histidine and zinc (II) nitrate will need to produce a strong acid (nitric acid). Hence, the reaction equilibrium is not favored for the forward reaction and KOH was added to neutralize the acid produced during the reaction. The molar ratio of Zn(II) to histidine is also very important. If the molar ratio of  $\text{Zn}(\text{NO}_3)_2 \cdot 6\text{H}_2\text{O}$  to histidine is 1:1, no solid products were obtained. We found out the best molar ratio of  $\text{Zn}(\text{NO}_3)_2 \cdot 6\text{H}_2\text{O}$  to histidine is 1.6:1. We also used different reaction temperatures (25, 70, 90, 110, 120, and 130 °C) and reaction times (24, 36, 48, 72, and 144 hours) for the syntheses of ZnMOF-1. Generally, ZnMOF-1 can be made at temperatures above 100 °C and with a Zn: histidine molar ratio

of 1.6:1. In a typical synthesis, ZnMOF-1 can be made by heating the reaction mixture at 130 °C for 48 hours.

Because single crystals of ZnMOF-1 made from hydrothermal reactions were not big enough for single-crystal X-ray diffraction studies, the layering method (solvent diffusion) was used to grow big crystals of ZnMOF-1. 20 mL of 0.2 M  $\text{Zn}(\text{NO}_3)_2$  solution was made by dissolving  $\text{Zn}(\text{NO}_3)_2$  in anhydrous methanol, and 20 mL of 0.2 M L-histidine solution was made by dissolving L-histidine in DI water. The L-histidine aqueous solution was added to the bottom of a thin glass tube. Then, various amount (0.6-1.2 mL) of KOH solution was added on top of the L-histidine aqueous solution. This was followed by adding a layer of anhydrous methanol, which served as a separation of the two reactants. Finally,  $\text{Zn}(\text{NO}_3)_2$  methanol solution was added on to the anhydrous methanol layer in the tube. The tubes were then placed under room temperature for 72 hours. However, this method did not yield any crystals.

In addition to the hydrothermal method and the layering method, we also tried to grow large crystals of ZnMOF-1 using the solvothermal method. Same mole ratio of zinc (II) nitrate and L-histidine was used as those in the hydrothermal method. Zinc(II) nitrate hexahydrate was preheated at 150 °C for 2 hours to remove the water in the compound. Anhydrous methanol was used as the solvent for the solvothermal reaction. The products from the solvothermal reactions are orange plate-like solids. However, the PXRD pattern of this product is different from that of ZnMOF-1, and only showed one strong peak around  $2\theta = 2^\circ$ , which was likely from the background. Other peaks were very weak.

As mentioned in the introduction, there is more than one type of CA available in nature. This implies that the active center of MOF should not be limited to zinc. For

example, Zhang<sup>14</sup> et al. synthesized a cobalt-centered novel material (Co-2,6-bis(2-benzimidazolyl) pyridine), which mimicked the active site of CA. Theoretically, transitional metals other than Zn should have the possibility to mimic CA as well. Thus, in order to make new MOFs mimicking CA, a similar methodology was applied to Ni(NO<sub>3</sub>)<sub>2</sub>·6H<sub>2</sub>O, Cu(NO<sub>3</sub>)<sub>2</sub>·2.5H<sub>2</sub>O, Co(NO<sub>3</sub>)<sub>2</sub>·6H<sub>2</sub>O, and FeCl<sub>2</sub>·4H<sub>2</sub>O in substitute of Zn(NO<sub>3</sub>)<sub>2</sub>·6H<sub>2</sub>O. However, the results were either no solid precipitates or no crystals from those reactions. For instance, using copper (II) nitrate as the reactant under the same conditions as that of ZnMOF-1 resulted in black solids. It is likely that the Cu(II) was reduced to copper metal by the histidine under the reaction condition.

The IR spectrum of ZnMOF-1 suggested the existence of functional groups in its structure, such as N-H stretching at 3225 cm<sup>-1</sup>, intramolecular -OH stretching at 3195 cm<sup>-1</sup>, cyclic C=C stretching at 1581 cm<sup>-1</sup>, carbonyl O-H bending at 1451 cm<sup>-1</sup>, and Zn-O stretching at 664 cm<sup>-1</sup>. These signals showed the presence of L-histidine in ZnMOF-1, as well as the linkage between zinc and oxygen from L-histidine.

To investigate if ZnMOF-1 can mimic the catalytic center of CA, the *p*-NPA hydrolysis reactions were studied with and without the ZnMOF-1 catalyst. As the results indicated, ZnMOF-1 catalyzed reaction had a higher reaction rate than the blank control, in which no catalyst was added. This result suggested that ZnMOF-1 has the catalytic ability to catalyze the *p*-NPA hydrolysis reactions and can mimic CA. Moreover, the thermal stability of ZnMOF-1 was tested with a thermogravimetric analyzer and had shown excellent stability. The TGA curve suggested that ZnMOF-1 can remain stable between room temperature and 400 °C. This is a sign that our MOF could function properly in this temperature range. Considering the condition for the typical application of biomimicking

MOF, 400°C can satisfy most of the thermostability needs. Additionally, the stability of the catalysts in a HEPES buffer solution (pH=8) was also examined. The retrieved catalyst was proved to be stable under the reaction condition. It showed a good recycling rate of 76% and excellent stability in the catalyzing environments.

## CONCLUSION

In this research, a novel zinc-based MOF mimicking the catalytic center of carbonic anhydrase has been synthesized using  $\text{Zn}(\text{NO}_3)_2 \cdot 6\text{H}_2\text{O}$  and L-histidine. Its catalytic ability was examined through the hydrolysis reaction of *p*-NPA, and the reaction rate of catalyzed reaction was more than twice of the uncatalyzed reaction. In addition, ZnMOF-1 possessed great stability in HEPES buffer (pH = 8). About 76% of the original amount was recovered after a 2-hour reaction. ZnMOF-1 can be thermally stable up to 400 °C.

The growth of big single crystals of ZnMOF-1 has been the biggest challenge in this research. We were unable to grow crystals large enough for single crystal X-ray studies. However, the TGA and CHN elemental analysis have confirmed the formula of ZnMOF-1. Additional research is needed to investigate the crystal structure of ZnMOF-1 and its activities to convert  $\text{CO}_2$  under commercial conditions.

## REFERENCES

1. Goeppert, A.; Czaun, M.; Prakash, G. K. S.; Olah, G. A. Air as the renewable carbon source of the future: an overview of CO<sub>2</sub> capture from the atmosphere. *Energy Environ. Sci.* 2012, 5, 7833-7853.
2. Lillerud, K; Olsbye, U; Tilset, M. Designing heterogeneous catalysts by incorporating enzyme-like functionalities into MOFs. *Top Catal.* 2010, 53: 859-868.
3. Zhang, X; Eldik, R. A functional model for carbonic anhydrase: thermodynamic and kinetic study of a tetraazacyclododecane complex of zinc(II). *Inorg. Chem.* 1995, 34, 22, 5606–5614.
4. Marino, T; Russo, N; and Toscano, M. A Comparative Study of the Catalytic Mechanisms of the Zinc and Cadmium Containing Carbonic Anhydrase. *J. Am. Chem. Soc.* 2005, 127, 12, 4242–4253.
5. Bräuer, M; P-L, J; Weston, J; Ernst Anders, A. Quantitative Reactivity Model for the Hydration of Carbon Dioxide by Biomimetic Zinc Complexes. *Inorg. Chem.* 2002, 41, 6, 1454–1463.
6. Rains, J; Donnelly, K; Oliver, T; Woscholski, R; Long, N; Barter, L. Bicarbonate Inhibition of Carbonic Anhydrase Mimics Hinders Catalytic Efficiency: Elucidating the Mechanism and Gaining Insight toward Improving Speed and Efficiency. *ACS Catalysis.* 2019, 9, 2, 1353-1365.

7. Power, I; Harrison, A; Dipple, G. Accelerating Mineral Carbonation Using Carbonic Anhydrase. *Environ. Sci. Technol.* 2016, 50, 5, 2610–2618.
8. Jin, C; Zhang, S; Zhang, Z; Chen, Y. Mimic carbonic anhydrase using metal-organic frameworks for CO<sub>2</sub> capture and conversion. *Inorg. Chem.* 2018, 57, 2169-2174.
9. Huang, Y.; Zhang, S.; Chen, H.; Zhao, L.; Zhang, Z.; Cheng, P.; Chen, Y., A Zinc Coordination Complex Mimicking Carbonic Anhydrase for CO<sub>2</sub> Hydrolysis and Sequestration. *Inorganic Chemistry* **2019**, 58 (15), 9916-9921.
10. Pan, Y; Liu, Y; Zeng, G; Zhao, L; Lai, Z. Rapid synthesis of zeolitic imidazolate framework-8 (ZIF-8) nanocrystals in an aqueous system. *Chem. Comm.*
11. Ren, S; Li, C; Tan, Z; Hou, Y; Jia, S; Cui, J. Carbonic anhydrase@ZIF-8 hydrogel composite membrane with improved Recycling and stability for efficient CO<sub>2</sub> capture. *J. Agric. Food Chem.* 2019, 67, 3372-3379.
12. Floyd, W; Baker, S; Valdez, C; Stolaroff, J; Bearinger, J; Satcher, J; Aines, R. Evaluation of a Carbonic Anhydrase Mimic for Industrial Carbon Capture. *Environ. Sci. Technol.* 2013, 47, 17, 10049–10055.
13. Sowri Babu, K., Ramachandra Reddy, A., Sujatha, C. et al. Synthesis and optical characterization of porous ZnO. *J Adv Ceram* 2, 260–265 (2013).
14. Zhang, Y; Wang, H; Zhou, S; Wang, J; He, X; Liu, J; Zhang, Y. Biomimetic material functionalized mixed matrix membranes for enhanced carbon dioxide capture. *J. Mater. Chem. A*, 2018, 6, 15585.